Control of a 750kW Permanent Magnet Synchronous Motor

Liping Zheng* and Dong Le
Calnetix Technologies, LLC
Cerritos, CA, USA
*lzheng@calnetix.com

***Abstract*— Permanent magnet synchronous motors have been widely used due to their high performance and high efficiency. In this paper, we talk about the control of a 750kW permanent magnet synchronous generator which is used for a hybrid turbocharger for a marine application. The controller outputs regulated 700V dc bus voltage with a voltage variation of less than 5% under 100% load transient condition to ensure that the inverter which relies on this 700V input will provide stable three-phase ac power output. The system overview, control methodology and control simulation using Matlab/Simulink is provided in detail. The tests and simulation results are also provided and compared to show the validation of the simulation model and the performance of the generator control and dc bus regulation.**

Keywords*— *DC Bus Voltage Regulation, Motor Control, Permanent Magnet Synchronous Motor, Sensorless

I. Introduction

Permanent magnet synchronous motors (PMSM) are getting widely used in many industrial applications. This has been made possible with the advent of high performance permanent magnets with high energy density and high operating temperature, providing the PMSM with industry leading power density and efficiency. The sensorless control is also very popular for high performance PMSM control. The position sensors or rotational transducers not only increase cost, maintenance, and complexity but also impair robustness and reliability of the drive system. Long cable length between the variable speed drive (VSD) and motor also makes it less attractive to use position sensors. Various sensorless control methods have been developed to provide high performance control [1-4].

This paper describes a new sensorless control method for high performance and very stable regulated voltage output. A method for initial position and speed estimation is also provided. In addition, the new control is not sensitive to the parameters variation such as induced back electromagnetic force (EMF), winding resistance and inductance.

II. System Overview

The overall system diagram is shown in Fig. 1. The PMSM which is shown in Fig. 2 is attached to the turbocharger of a diesel engine. The specification of PMSM is shown in Table I. The inverter is used to convert the power from 700Vdc voltage to three-phase 440V /60 Hz ac grid. The VSD/converter, which is the main focus of this paper, is used to convert generator high frequency ac power to 700V dc power.

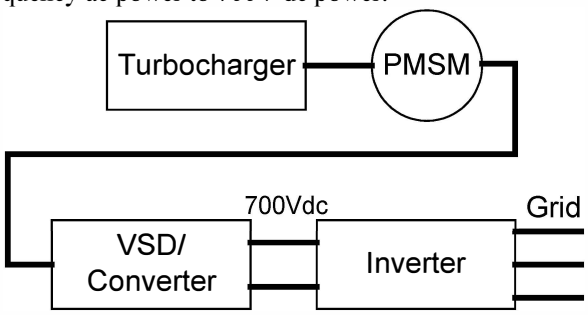

Fig. 1. Overall system diagram.

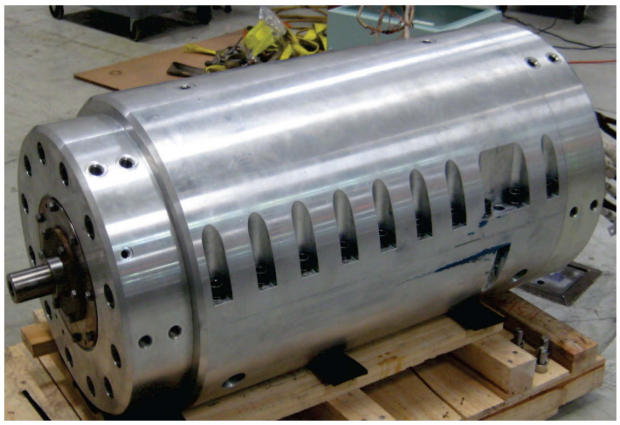

Fig. 2. Picture of the prototype PMSM.

TABLE I
Specification of the PMSM

Name	Value
Nominal Speed	9,500 rpm
Nominal Power	750 kW
D-axis Inductance	18 μH
Q-axis Inductance	18 μH
Line-line resistance	0.95 mΩ

The prototype of the designed converter, shown in Figure 3, includes three sections. The left section is the input section, which has a programmable logic controller (PLC) and display, a main contactor, and the pre-charge circuits. The middle section has line reactors which are used to reduce switching harmonics and also to provide load sharing between three parallel switching devices. The right section is the main power converting section which includes main control circuits, pulse-width

modulation (PWM) switching IGBT bridges and dc link capacitors.

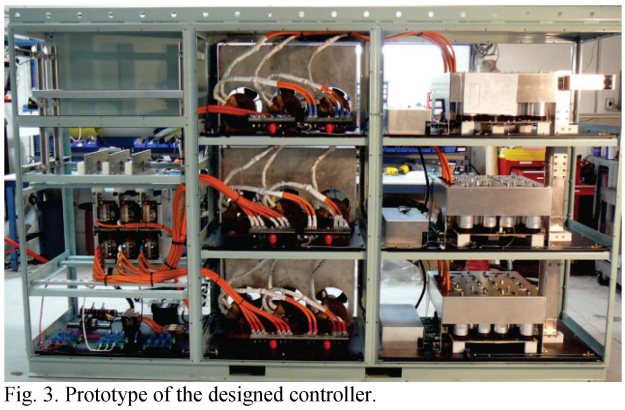

Fig. 3. Prototype of the designed controller.

III. System Control Scheme

The simplified control scheme is shown in Fig. 4. The block bc/qd is used to convert three-phase currents to qd-axis currents. The current regulation block is used to regulate d-axis and q-axis currents independently. The PWM block is a space vector pulse width modulation block, which converts q-axis and d-axis voltage signals to the switching on-off time of each IGBT. The catch spin & initial angle detection block is used to detect generator speed and initial angle during start-up.

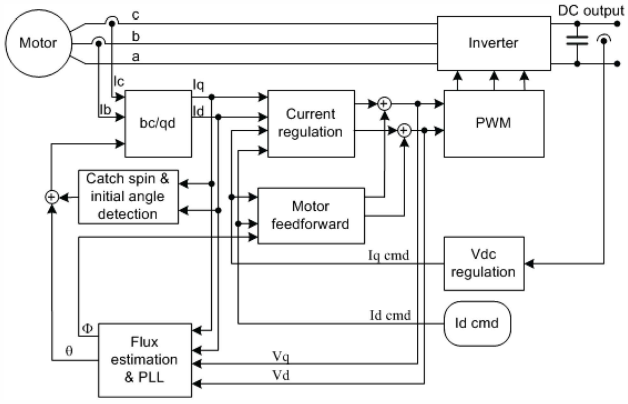

Fig. 4. Simplified control scheme.

During normal operation, d-axis current command (Id cmd) is set to zero, and q-axis current command (Iq cmd) is controlled by the output of the Vdc regulation block. If the DC bus voltage is lower than the voltage setting of 700V, the vdc regulation block will output negative Iq command. If the DC bus voltage is higher than the voltage setting of 700V, the Vdc regulation block will automatically output positive Iq command. A negative Iq command will generate power from the motor while a positive Iq command will automatically do motoring to convert input electric power to kinetic energy.

A. Dq0 transformation

Park's transformation is used to convert stationary reference frame signals to orthogonal rotational reference frame signals. The three-phase abc signals and qd-axis used in the motor/generator controller are shown in Fig. 5. The d-axis is 90 electrical degrees behind of q-axis. The angle, θ, is the angle between the q-axis of the rotating axis and a-axis of the stationary abc-axis. The phase current is positive when motoring, and negative when generating.

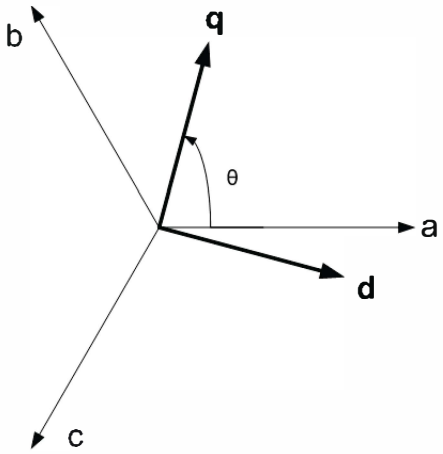

Fig. 5. Three-phase and qd axis.

The relationship between the abc-axis and the dq-axis is shown in the following equations, where S represents any of the variables (current, voltage, flux linkage,...).

$$\begin{aligned} S_a &= S_q\cos(\theta) + S_d\sin(\theta) \\ S_b &= S_q\cos(\theta-\frac{2\pi}{3}) + S_d\sin(\theta-\frac{2\pi}{3}) \\ S_c &= S_q\cos(\theta+\frac{2\pi}{3}) + S_d\sin(\theta+\frac{2\pi}{3}) \end{aligned} \quad (1)$$

$$\begin{aligned} S_q &= \frac{2}{3}\left[S_a\cos(\theta) + S_b\cos(\theta-\frac{2\pi}{3}) + S_c\cos(\theta+\frac{2\pi}{3})\right] \\ S_d &= \frac{2}{3}\left[S_a\sin(\theta) + S_b\sin(\theta-\frac{2\pi}{3}) + S_c\sin(\theta+\frac{2\pi}{3})\right] \end{aligned} \quad (2)$$

B. Motor feed forward

The voltage equations of PMSM in the rotational reference frame can be expressed as [5]:

$$\begin{aligned} V_q &= R_s I_q + \frac{d\lambda_q}{dt} + \lambda_d\frac{d\theta_r}{dt} \\ V_d &= R_s I_d + \frac{d\lambda_d}{dt} - \lambda_q\frac{d\theta_r}{dt} \end{aligned} \quad (3)$$

where Vq, Vd, Iq, Id, λq, and λd are q-axis and d-axis components of voltage, current and flux linkage respectively. θr is the rotor angle.

At steady state, equ. (3) will yield to (4), which can be used as feed forward equations.

$$\begin{aligned} V_q &= R_s I_q + \omega_e L_d I_d + E_f \\ V_d &= R_s I_d - \omega_e L_q I_q \end{aligned} \quad (4)$$

C. Catch-spin operation

For sensorless control, it is still challenging to accurately detect the initial frequency and angle of the spinning machine for flying catch. There is much literature talking about initial speed detection [6-8]. The method developed here is based on the theory that the change of current through inductance is proportional to

the applied voltage and time, and inversely proportional to the inductance.

The typical schematic of the 2-level PWM output and the motor/grid is shown in Fig. 6, where switches S1-S6 are power switching devices. The line inductances L1-L3 are used to reduce current harmonics and are optional.

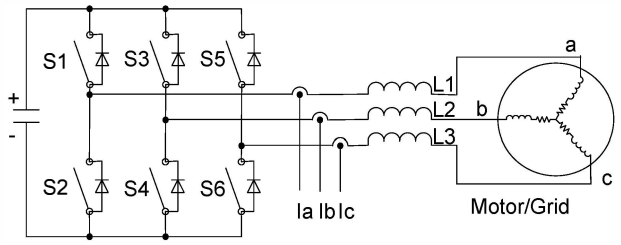

Fig. 6. Typical schematic of the 2-level PWM output and the motor/grid.

Assuming the motor has the three-phase open circuit voltage as shown below:

$$V_a = V_m \cos(\omega t + \theta)$$
$$V_b = V_m \cos\left(\omega t + \theta - \frac{2\pi}{3}\right) \quad (5)$$
$$V_c = V_m \cos\left(\omega t + \theta + \frac{2\pi}{3}\right)$$

If the bottom three switches (S2, S4 and S6) close for a period of time Δt, the final current flow through phase a, b, and c will be

$$I_a = \frac{\Delta t}{L_s} V_m \cos(\omega t + \theta)$$
$$I_b = \frac{\Delta t}{L_s} V_m \cos\left(\omega t + \theta - \frac{2\pi}{3}\right) \quad (6)$$
$$I_c = \frac{\Delta t}{L_s} V_m \cos\left(\omega t + \theta + \frac{2\pi}{3}\right)$$

From (6), at time t=0, we have,

$$V_m = \sqrt{I_a^2 + \frac{(I_b - I_c)^2}{3}}$$
$$\theta = \tan^{-1}\left(\frac{I_b - I_c}{\sqrt{3} I_a}\right) \quad (7)$$

The frequency (ω) can be easily calculated from V_m based on the known back EMF constant.

After initial estimation, further refining of the speed and angle is required to accurately estimate the speed and angle.

D. Flux Estimation and PLL

Flux estimation is the key part of sensorless motor control. The performance of flux estimation directly affects the system performance of the motor control. Virtual flux estimation together with phase lock loop (PLL) is used to provide reliable position and speed estimation. The virtual flux estimator uses q and d axes components of voltage command and current feedback to estimate the position and speed. By using PLL, the flux can be tracked smoothly, thus the position noise due to arc-tangent function is greatly reduced.

IV. Simulation

The control scheme has been verified using Matlab/Simulink simulations. Fig. 7 shows the simulation model.

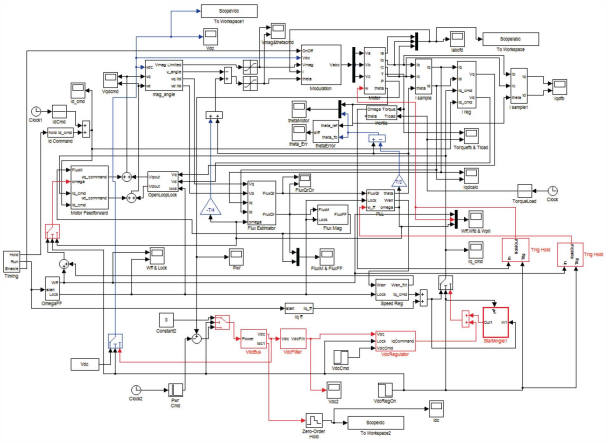

Fig. 7. Simulation model.

Fig. 8 and Fig. 9 show the simulated dc bus voltage response and phase current waveforms when a step load of 0% to 100% applied at the time of 0 seconds. The results show that the dc bus voltage dip is below 5%.

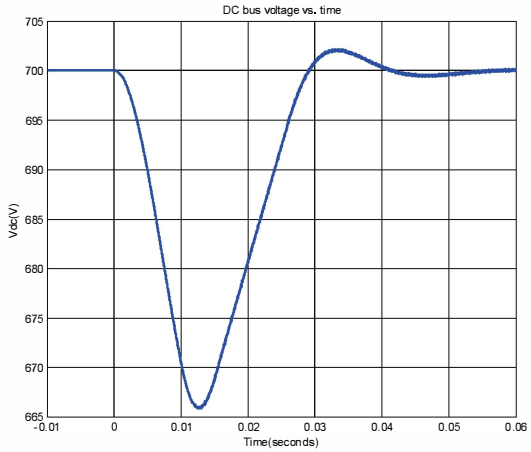

Fig. 8. DC bus voltage overshoot when step load from 0 kW to 750 kW at 10,000 rpm.

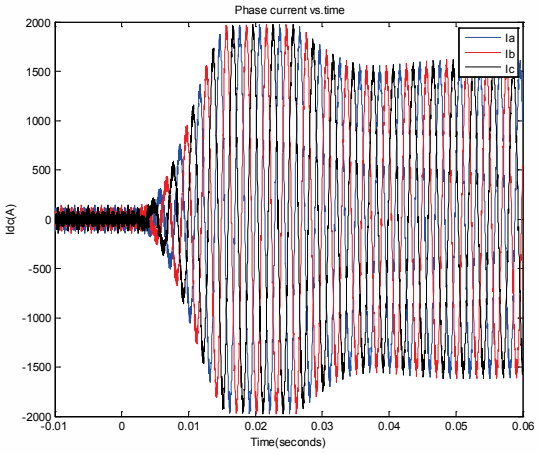

Fig. 9. Phase current waveforms when step load from 0 kW to 750 kW at 10,000 rpm.

Fig. 10 and Fig. 11 show the dc bus voltage response and phase current waveforms when a step load of 100 % to 0% is applied at the time of 0 seconds. The result also shows that the dc bus voltage overshoot is below 5%.

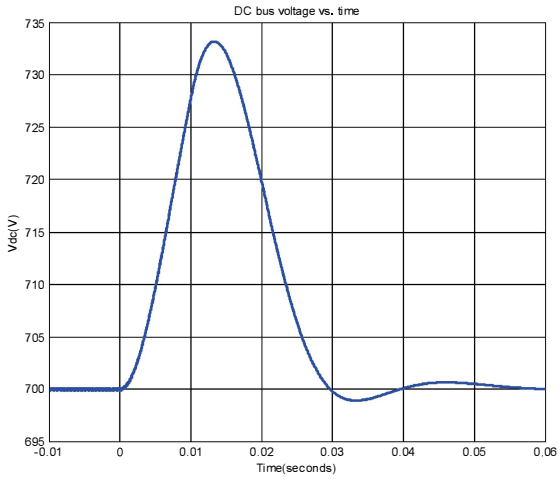

Fig. 10. DC bus voltage overshoot when step load from 750 kW to 0 kW at 10,000 rpm.

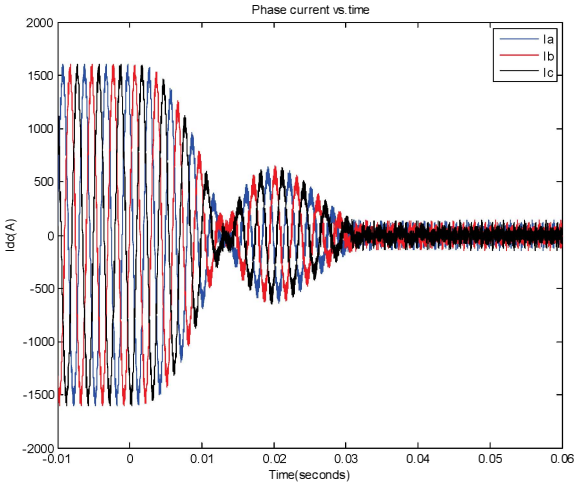

Fig. 11. Phase current waveforms when step load from 750 kW to 0 kW at 10,000 rpm.

V. Test Results

Catch-spin performance was tested at different initial speed conditions (shown in Table II). From these results we can see that the speed error is less than 5%. The detected speed error is lower at higher speeds because of the higher current signal to noise ratio at higher speeds.

TABLE II
CATCH SPIN RESULTS

Actual Speed (rpm)	Speed Initial Est (rpm)	Speed Refined (rpm)	Refined Error (%)
10000	8962	10117	1.2
10000	8475	10146	1.5
10000	8795	10032	0.3
10000	8847	10160	1.6
10000	8757	10141	1.4
5400	5300	5601	3.7
5113	5295	4889	-4.4
4900	5061	5138	4.8
4745	5166	4870	2.6

Fig. 12 shows the phase current waveform when catch-spinning and then boosting the dc bus voltage to the rated voltage of 700V.

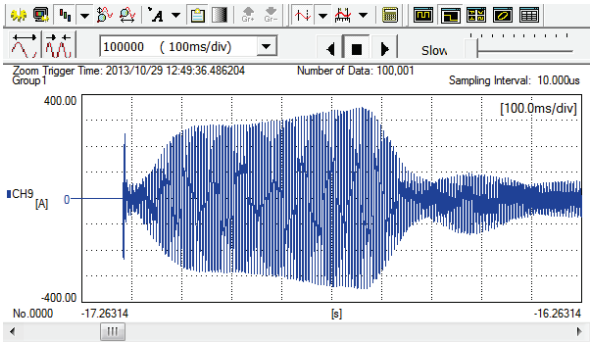

Fig. 12. Current waveform when catch -spinning and then boosting dc bus voltage to the rated 700V.

The DC bus voltage variations under transient load conditions were tested at 580 kW load condition and compared with simulated results. Fig. 13 to Fig. 15 show simulation results and actual test results of the step load response of the dc bus voltage and phase current when the external load changes from 0 kW to 580 kW. The results show that the simulation and actual test results match very well.

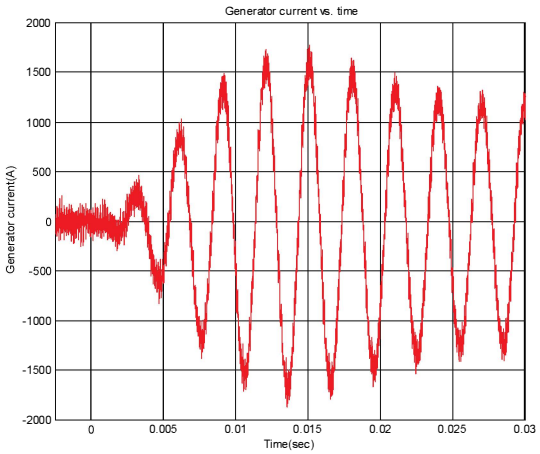

Fig. 13. Measured phase current when the load changed from 0 to 580 kW at 10,000 rpm.

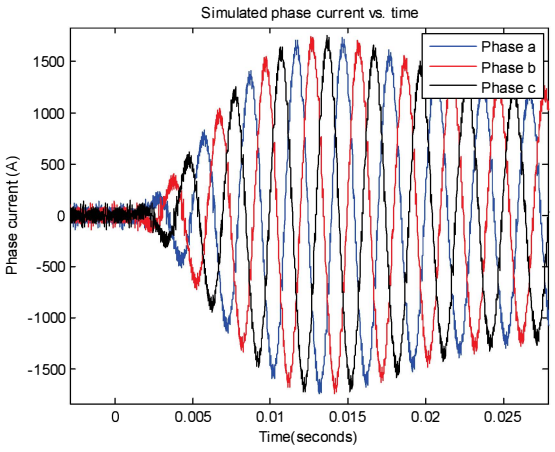

Fig. 14. Simulated phase current when load changes from 0 to 580 kW at 10,000 rpm.

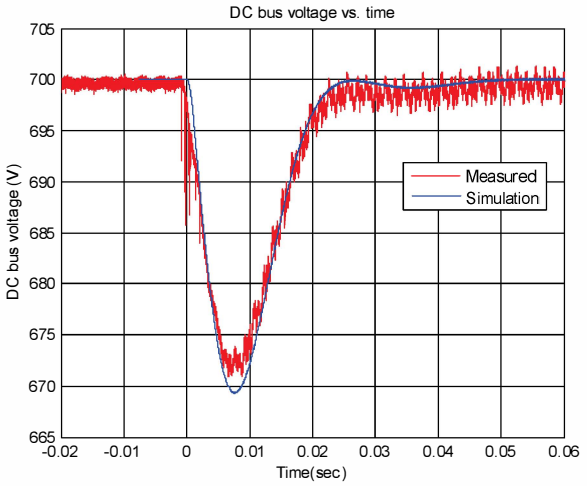

Fig. 15. DC bus voltage dip when step load from 0 to 580kW at 10,000 rpm.

Fig. 16 shows the measured and simulated dc voltage waveforms when the 580 kW load is removed at time 0. Fig. 15 and Fig. 16 show that transient response of the dc bus voltage is less than 5%.

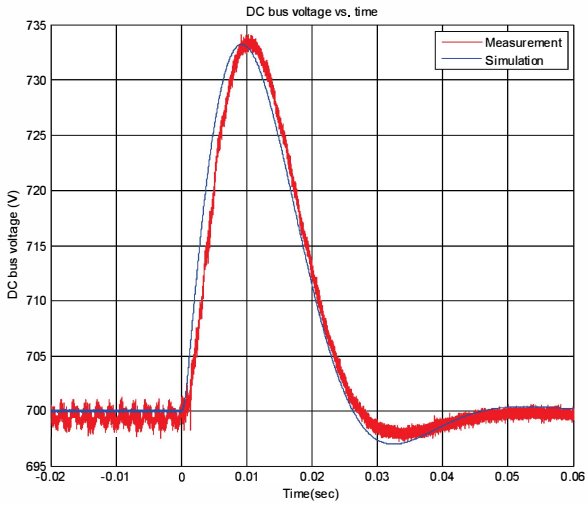

Fig. 16. DC bus voltage overshoot when step load from 580kW to 0 kW at 8,000 rpm.

VI. Conclusion

The control of a 750kW permanent magnet synchronous generator which is used for marine hybrid turbocharger applications has been proposed to meet the tough requirement of less than 5% dc bus voltage variation under transient load condition. The system overview, control methodology, and control simulation using Matlab/Simulink has been conducted to provide simulation results that meet system performance requirements. Comparison of the tests and simulation results show the validation of the simulation model and the promising performance of the generator control and dc bus voltage regulation, meeting the performance requirements of the system.

References

[1] B. Bae, S. Sul, J. Kwon, and J. Byeon, "Implementation of Sensorless Vector Control for Super-High-Speed PMSM of Turbo-Compressor," *IEEE Trans. on Industry Applications,* vol. 39, no. 3, pp. 811-818, 2003.

[2] J. X. Shen, Z. Q. Zhu, and D. Howe, "Improved Speed Estimation in Sensorless PM Brushless AC Drives," *IEEE Trans. on Industry Applications,* vol. 38, no. 4, pp. 1072-1080, 2002.

[3] I., S. Tomita, M. Doki, S. Okuma, S. "Sensorless Control of Permanent-Magnet Synchronous Motors Using Online Parameter Identification Based on System Identification Theory" *IEEE Trans. Ind. Applications,* 2006, vol.53, no.2, pp.363-372, 2006.

[4] J. H. Kim, S. Lee, R. Y. Kim, and D. S. Hyun, "A Sensorless Control using Extended Kalman Filter For an Interior Permanent Magnet Synchronous Motor Based on an Extended Rotor Flux," *IEEE 38th Annual Conf. on Industrial Electronics Society,* Oct. 2012.

[5] Chee-mun Ong, *Dynamic Simulation of Electric Machinery Using Matlab/Simulink*, Prince Hall PTR, 1997.

[6] M. Tursini, R. Petrella, and F. Parasiliti, "Initial Rotor Position Estimation Method for PM Motors," *IEEE Trans. Ind. Applications,* vol.39, no.6, pp.1630-1640, 2003.

[7] P. B. Schmidt, M. L. Gasperi, G. Ray, and A. H. Wijenayake, "Initial rotor angle detection of nonsalient pole permanent magnet synchronous machine," *IEEE-IAS Annual Meeting,* pp. 459–463, New Orleans, 1997.

[8] T. Noguchi, K. Yamada, S. Kondo, and I. Takahashi, "Initial Rotor Position Estimation Method of Sensorless PM Synchronous Motor with No Sensitivity to Armature Resistance," *IEEE Trans. on Industry Electronics*, vol. 45, no.1, pp. 118-125, 1998.